

POST-BUCKLING BEHAVIOUR AND STRENGTH OF ANGLE COLUMNS

Pedro B. Dinis, Dinar Camotim and Nuno Silvestre

Civil Engineering Department, ICIST/IST, TU Lisbon, Av. Rovisco Pais, 1049-001 Lisboa, Portugal
e-mails: dinis@civil.ist.utl.pt, dcamotim@civil.ist.utl.pt, nunos@civil.ist.utl.pt

Keywords: Thin-walled angle columns, Post-buckling behaviour, Ultimate strength, Shell finite element analysis, Generalised Beam Theory (GBT).

Abstract. *This paper reports the available results of an ongoing numerical investigation aimed at providing fresh insight on the mechanics underlying the local and global post-buckling behaviour of short-to-intermediate equal-leg angle steel columns. Both pinned-ended and fixed-ended columns are analysed and the most of the results presented and discussed concern their elastic buckling and (mostly) post-buckling behaviour – moreover, the elastic-plastic load-carrying capacity of these columns is also briefly addressed, as well as the corresponding design implications. The numerical post-buckling and ultimate strength results presented were obtained by means of ABAQUS shell finite element analyses. In order to help clarifying the distinction between local and global buckling, some GBT-based critical stresses and buckling mode shapes are also displayed and interpreted.*

1 INTRODUCTION

It is well known that thin-walled members having cross-sections with all their wall mid-lines intersecting at a single point (e.g., angle, T-section or cruciform members) exhibit no primary warping – the cross-section warping resistance stems exclusively from secondary (across the thickness) warping. This feature automatically implies an extremely low torsional stiffness, thus rendering these thin-walled members highly susceptible to buckling phenomena involving torsion (torsional or flexural-torsional buckling). Moreover, in members with the above cross-section shapes and short-to-intermediate lengths it is often hard to separate the torsion and local deformations and, thus, to distinguish between local and global buckling – these members commonly exhibit “mixed” local/torsional buckling mode shapes. Since the above two instability phenomena are associated with markedly different post-critical behaviours (strength reserves), it is fair to say that this distinction may have far-reaching implications on the definition of a rational structural model capable of providing accurate ultimate strength estimates for such members.

The post-buckling behaviour and strength of angle and T-section columns, beams and beam-columns has attracted the attention of several researchers in the past (e.g., [1-4]). More recently, thorough studies of the buckling behaviour of angle beams and beam-columns with equal and unequal legs led Trahair [5, 6] to propose some modifications to the currently available design rules. Mohan *et al.* [7] carried out a numerical and experimental investigation on the flexural and local buckling behaviour of angle members belonging to lattice tower K-panels. Moreover, Young [8], Ellobody and Young [9] and Rasmussen [10, 11] performed extensive experimental tests and shell finite element analyses aimed at obtaining ultimate loads of fixed-ended angle columns, and compared their results with the predictions yielded by currently available design rules. It is worth noting that Rasmussen [11] proposed an approach based on the Direct Strength Method (DSM – e.g., [12]) to design angle columns, which adopts the DSM global design curve to estimate the column flexural and local strengths – in the latter case, the use of the global curve is combined with effective cross-section properties. More recently, Chodraui *et al.* [13, 14] proposed a slightly different DSM-based design approach for angle columns, which differs from the previous one in the fact that the column global strength is taken as the lower of the flexural and torsional values, both obtained with the same (global) DSM design curve. Finally, a recent numerical investigation, carried out by means of Generalised Beam Theory (GBT) analyses, shed some new light on how to characterise and/or distinguish between local and global buckling in angle, T-section and cruciform thin-walled members (columns, beams and beam-columns) [15].

Moreover, the authors suggested that a design curve for such members should be based on global (torsional) buckling concepts, namely by using the gross cross-section properties – recall that recent design proposals [10, 11, 13, 14] are based on local buckling concepts (they involve effective cross-section calculations). In order to confirm this assertion, it is necessary to investigate the post-buckling behaviour and ultimate strength of the members under scrutiny – a first step towards achieving this goal was made by the authors [16, 17], who analysed the elastic post-buckling behaviour of simply supported equal and unequal-leg angle columns. The aim of the work reported in this paper is to extend the above investigation, by analysing also the elastic behaviour and elastic-plastic strength behaviour of both simply supported (pinned-ended) and fixed-ended equal-leg angle columns.

The numerical results presented and discussed concern thin-walled steel ($E=210\text{ GP}$ and $\nu=0.3$) angle columns exhibiting (i) pinned and fixed ends, (ii) equal legs ($70\times 70\text{ mm}$ and $t=1.2\text{ mm}$ – the effect of rounded corners is disregarded), (iii) short-to-intermediate lengths and (iv) various yield-to-critical stress ratios – all columns analysed contain critical-mode geometrical imperfections with very small amplitudes (10% of the wall thickness t). Almost all the numerical results were obtained through ABAQUS [18] shell finite element analyses, (i) adopting column discretisations into fine 4-node isoparametric element meshes (length-to-width ratio close to l) and (ii) modelling the column end supports either by imposing null transverse displacements at all end section nodes (pinned supports – P condition) or by attaching rigid end-plates to the end section centroids (fixed supports – F condition) – accounts of all the column finite element modelling issues can be found in [19, 20]. Moreover, in order to characterise and distinguish between local and global buckling of angle columns, GBT analyses are also performed using the GBTUL code [21, 22]. The paper displays results concerning the column (i) elastic buckling and (mostly) post-buckling behaviours, and (ii) elastic-plastic ultimate strength – they include curves and/or diagrams providing the evolution of the column deformed configuration and longitudinal normal stresses along a given equilibrium path.

2 BUCKLING BEHAVIOUR – COLUMN LENGTH SELECTION

The curves shown in figure 1(a) provide the variation, with the column length L (logarithmic scale), of the ABAQUS critical load P_{cr} , both for pinned-ended (P curve) and fixed-ended (F curve) angle columns – this figure also depicts single half-wave buckling loads, $P_{b,1}$, yielded by GBT analyses and including 7 deformation modes: 4 global (1-4) and 3 local (5-7). As for figures 1(b₁)-(b₂), they display the GBT-based modal participation diagrams for columns with both end support conditions – they provide the contributions of each GBT deformation mode to the column buckling modes. Finally, figure 1(c) shows the buckling mode shapes yielded by the GBT analyses for the pinned-ended columns with $L=20, 98, 365, 1000\text{ cm}$, as well as the in-plane shapes of the first 5 deformation modes (axial extension excluded). These buckling results prompt the following remarks:

- (i) Both the pinned and fixed-ended columns display similar buckling features (obviously, the fixed-ended P_{cr} values are generally higher than their simply supported counterparts): (i₁) P_{cr} decreases monotonically with L and corresponds to *single half-wave* buckling (recall that similar curves concerning members with more complex cross-section shapes always exhibit local minima associated with local/distortional buckling involving growing half-wave numbers), (i₂) the GBT and ABAQUS results virtually coincide, and (i₃) the torsion mode 4 almost plays a key role, as it participates in the critical buckling modes of all but the very long columns.
- (ii) For the entire length range, the critical buckling modes of all pinned and fixed-ended angle columns involve just four deformation modes (2, 3, 4, 6) – note that (ii₁) the symmetric local mode 5 does not participate in any column critical buckling mode and (ii₂) the participations of the (non-torsional) modes 2 and 6 are smaller in the fixed-ended columns. For very short columns, buckling takes place in mixed local-torsional modes (4+6). Very short to short columns buckle in pure torsional modes (4). Intermediate columns buckle in mixed (major axis) flexural-torsional modes (2+4). The longer columns buckle in pure (minor axis) flexural modes (3).
- (iii) In order to investigate the column post-buckling behaviour, the eleven short-to-intermediate lengths indicated in figure 1(a) were selected. They correspond to columns that (iii₁) buckle in or around the “horizontal plateaus” of the P and F P_{cr} vs. L curves (pure torsional, local-torsional or flexural-torsional modes) and (iii₂) exhibit very similar mid-span cross section buckled shapes – see figure 1(c), concerning pinned-ended columns. The lengths selected are $L_1=20\text{ cm}$, $L_2=36\text{ cm}$, $L_3=53\text{ cm}$, $L_4=98\text{ cm}$, $L_5=133\text{ cm}$, $L_6=182\text{ cm}$, $L_7=252\text{ cm}$, $L_8=365\text{ cm}$, $L_9=532\text{ cm}$, $L_{10}=700\text{ cm}$ and $L_{11}=890\text{ cm}$ – eighth pinned-ended columns (L_7 - L_8 – $22.0\leq\sigma_{cr}\leq 30.9\text{ MPa}$) and nine fixed-ended columns (L_3 - L_{11} – $21.1\leq\sigma_{cr}\leq 27.5\text{ MPa}$) were analysed.

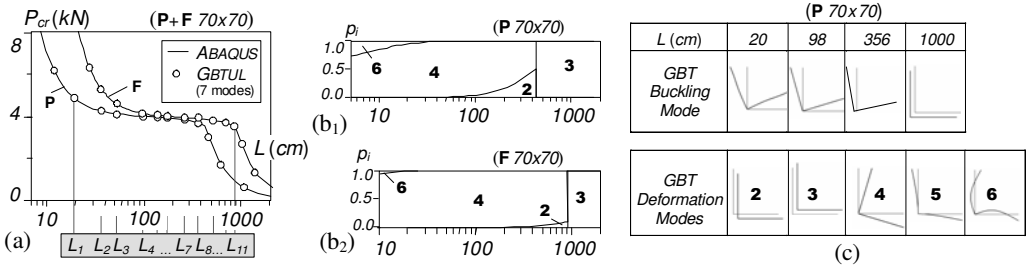


Figure 1: (a) P_{cr} vs. L curves and (b) GBT modal participation diagrams (pinned and fixed-ended columns), and (c) in-plane shapes of 4 buckling modes and first 5 GBT deformations modes (pinned-ended columns).

3 COLUMN POST-BUCKLING BEHAVIOUR

ABAQUS shell finite element analyses are employed to investigate the post-buckling behaviour of columns containing critical-mode initial imperfections with very small amplitudes (10% of the wall thickness $t=1.2mm$). The columns analysed exhibit (i) pinned or fixed end sections, (ii) the short-to-intermediate lengths indicated before and (iii) 5 yield-to-critical stress ratios ($f_y/\sigma_{cr} \approx 1.3, 2.5, 5.0, 9.8$ and ∞ – values corresponding to an “average” critical stress $\sigma_{cr}=24 MPa$ and viewing the elastic behaviour as associated with an infinite yield stress).

3.1 Elastic post-buckling behaviour

Post-buckling results concerning pinned-ended angles (P 70x70) with lengths L_1 to L_8 are first presented. Figures 2(a)-(b) show the upper parts of the column post-buckling equilibrium paths (i) P/P_{cr} vs. β , where β is the mid-span web chord rigid-body rotation, and (ii) P/P_{cr} vs. d/t , where d is the shear centre displacement absolute value. Figure 2(c) displays the L_3 and L_5 column deformed configurations at two β values. In order to clarify issues raised by the observation of the curves shown in figures 2(a)-(b), additional post-buckling results are presented in figure 3 – besides two equilibrium paths also included in figure 2(a), they consist of column mid and quarter-span cross-section deformed configurations. The observation of all these post-buckling results prompts the following comments:

- (i) The L_1 - L_8 column post-buckling behaviours (equilibrium paths) exhibit distinct characteristics: (i₁) while those concerning the L_1 - L_3 columns (local-torsional buckling) are clearly stable (fairly high post-critical strength) and involve minute mid-span cross-section shear centre displacements, (i₂) the L_5 - L_8 column post-buckling behaviours (flexural-torsional buckling) are only marginally stable (low post-critical strength and occurrence of limit points for moderate rotations) and involve considerable mid-span shear centre displacements. The L_4 column lays somewhere in between and may be viewed as a transition between the two previous behaviours.
- (ii) In the (intermediate) L_5 - L_8 columns the flexural-torsional deformed configuration “switches” abruptly from a single half-wave to three half-waves (see as fig. 2(c₂)) soon after the peak load is reached – these peak load and “deformed configuration switch” occur for gradually smaller β values as the column length increases ($L_5 \rightarrow L_8$). Such behavioural features are not exhibited by the (shorter) L_1 - L_3 columns. In order to try to explain the above differences, one looks at the L_3 and L_5 column post-buckling results shown in figure 3 – it is observed that:

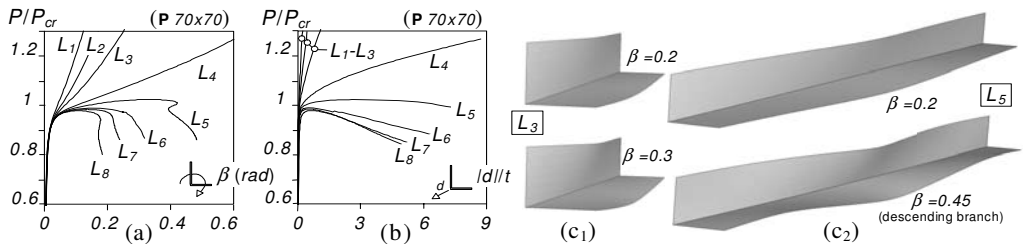


Figure 2: Pinned-ended columns: (a) P/P_{cr} vs. β and (b) P/P_{cr} vs. d/t equilibrium paths, and (c) column deformed configurations of the (c₁) L_3 and (c₂) L_5 columns at two equilibrium states.

- (ii.1) The third and fourth L_5 column mid and quarter-span cross-section deformed configurations, concerning the post-peak equilibrium states 3 and 4, exhibit significant amounts of (predominantly minor axis) flexure associated with tensile stresses in the cross-section corner regions – note that the flexural displacements are barely visible (but not null) in all the remaining (L_3 and L_5 column) deformed configurations. Moreover, these mid-span flexural displacements “overshadow” the corresponding torsional rotations along the equilibrium path descending branch – figure 3 shows that this descending branch is quite steep, which means that there is a small rotation increase.
- (ii.2) The GBT modal features help explaining the differences between the short and intermediate column post-buckling behaviours. The modal participation diagram given in figure 1(b₁) suggests that the amount of column post-buckling strength is directly related with the level of participations of modes 6 (local with inflection points) and 2 (major axis flexure) in the column buckling mode – recall that either of them is combined with the predominant torsional mode 4 (designated as “local” by Rasmussen [10], who views it as the simultaneous rotation of two pinned plate outstands). While the presence of mode 6 is responsible for a perceptible post-critical strength (short columns), the participation of mode 2 causes a destabilising effect leading to a limit point and a “deformed configuration switch” (intermediate columns).

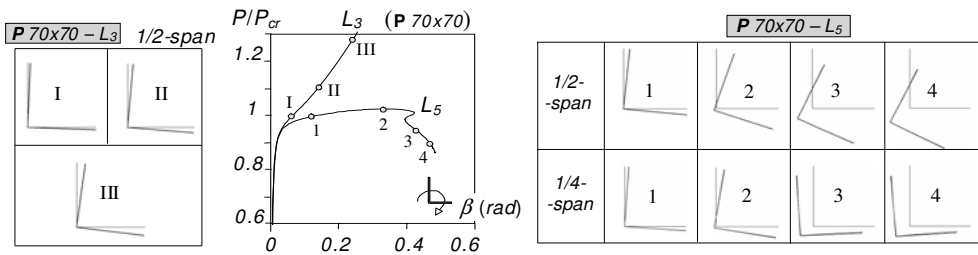


Figure 3: L_3 - L_5 columns: P/P_{cr} vs. β paths and cross-section deformed configuration evolution.

In order to acquire deeper insight on the above angle column post-buckling behaviours, one next investigates the longitudinal normal stress evolution of the L_3 - L_5 columns. The curves shown in figures 4(a) and 5(a) concern the mid-line normalised longitudinal normal stresses (σ/σ_{cr}) acting on the L_3 and L_5 column mid-span cross-sections at three applied load levels, corresponding to the equilibrium states indicated in the equilibrium paths located at the right hand side – also shown, below each stress distribution set, are the mid-span cross-section deformed configurations at the higher applied load ($P/P_{cr}=1.13$ and 1.02). Figures 4(b) and 5(b) show the variation of the higher load stress distributions between the column 1/8 and mid-span cross-sections. Finally, figure 6 compares the mid-span stress evolution of the L_3 - L_5 columns. After observing these results, it is possible to conclude that:

- (i) The mid-line normal stresses remain practically uniform up until $P/P_{cr} \approx 0.8$. As P increases, the stress distribution becomes progressively more non-uniform, with a quite different evolution for the L_3 and L_5 columns. Moreover, in both columns the longitudinal variation of the cross-section stress distribution is rather significant. A closer look at the two sets of stress distributions shows that:

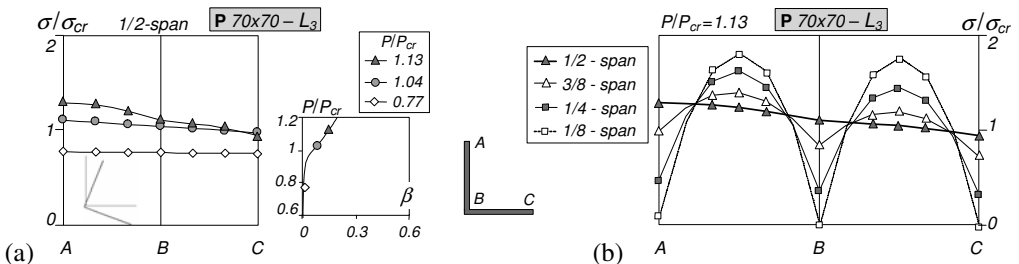


Figure 4: L_3 column (a) normal stress distribution evolution at the mid-span cross-sections and (b) normal stress distributions variation between the eighth and mid-span cross-sections ($P/P_{cr}=1.13$).

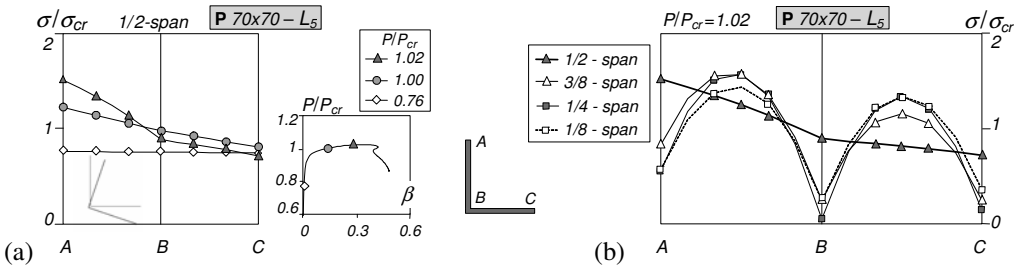


Figure 5: L_5 column (a) normal stress distribution evolution at the mid-span cross-sections and (b) normal stress distributions variation between the eighth and mid-span cross-sections ($P/P_{cr}=1.02$).

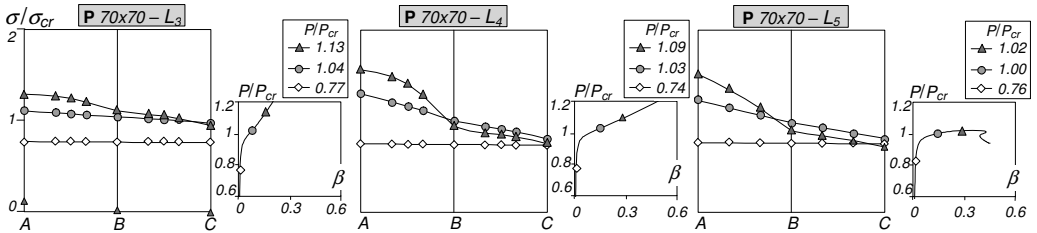


Figure 6: L_3 - L_5 column normal stress distribution evolution at the mid-span cross-sections.

- (i.1) At mid-span, the L_3 column stresses end up being (i₁) mildly non-uniform in the vertical leg (slightly non-linear distribution with higher value at the free edge) and (i₂) almost uniform in the horizontal leg (lower value at the free edge). The 1/8, 1/4 and 3/8-span stress distributions are highly non-linear in both legs (parabolic distribution – higher and lower values at the mid-points and corner) – these stresses decrease and become more asymmetric (lower values in the horizontal leg) as mid-span is approached.
- (i.2) At mid-span, the L_5 column stresses end up being (i₁) clearly non-uniform in the vertical leg (linear distribution with higher value at the free edge) and (i₂) mildly non-uniform in the horizontal leg (lower value at the free edge). The 1/8, 1/4 and 3/8-span stress distributions are qualitatively similar to the L_3 column ones (non-linear distribution with higher and lower values at the leg mid-points and corner) – in this case, these three stress distributions are equally asymmetric and, moreover, those concerning the 1/4 and 3/8-span cross-sections are practically identical (and a bit higher than the 1/8-span one).
- (ii) The L_1 - L_2 (short) and L_6 - L_8 (intermediate) column stresses are similar to those presented in figures 4(a)-(b) and 5(a)-(b) for the L_3 and L_5 columns, respectively. The L_4 column again corresponds to a transition between the two above column sets – this can be confirmed by looking at the L_3 - L_5 column mid-span stress evolutions displayed in figure 6. At this stage, it is worth noting that the stress distributions determined for either of the L_6 - L_8 columns are not in line with the widespread belief (*e.g.*, [10]) that buckled short-to-intermediate equal-leg angle columns exhibit the normal stress distribution sketched in figure 7 – each leg behaves like a pinned-free long plate (parabolic distributions with the higher value at the corner).

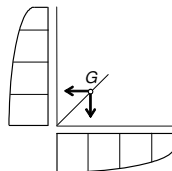


Figure 7: Typical equal-leg angle column normal stress distribution (each leg behaving like a pinned-free long plate).

- (iii) Since, in the authors’ opinion, the discrepancy between the determined and expected (widely accepted) equal-leg angle column post-buckling behaviours stems from the occurrence of bending, associated with the shear centre

displacements plotted in figure 2(b), it was decided to analyse the post-buckling behaviours of the L_5 - L_8 columns with the shear centre displacement d fully restrained (PR columns) – for comparison purposes, isolated plates with one longitudinal free edge and the remaining ones pinned (PP plates) and the dimensions of a leg (70 mm width, $t=1.2\text{ mm}$ thickness and the L_1 - L_8 lengths) were also analysed. Figure 8(a) shows the P/P_{cr} vs. β equilibrium paths of the PP plate and PR column with length L_5 (qualitatively similar results were obtained for the other lengths). Figures 8(b)-(c) display the PR column (iii₁) mid-span stress distribution evolution and (iii₂) stress distribution variation between the 1/8 and mid-span cross-sections for $P/P_{cr}=1.17$. The observation of this new set of results prompts the following remarks:

- (iii.1) The PP plates and PR columns share the same critical buckling stresses (up to 3.8% higher than the corresponding P columns) and post-buckling behaviours – see the coincident P/P_{cr} vs. β equilibrium paths and normal stress distribution evolutions in figures 8(a)-(b). Moreover, the PP plate stresses are equal to those acting on each PR column leg – see figure 8(c).
- (iii.2) Restraining the shear centre displacement, very meaningful in all intermediate P columns (see fig. 2(b)), significantly affects the corresponding post-buckling behaviours – they now are clearly stable and do not exhibit deformed configuration “switches” (*i.e.*, they “mimic” the PP plates).
- (iii.3) The shear centre displacement restraint also has marked impact on the column mid-span stress distributions, which now closely resemble those shown in figure 7 – *i.e.*, the two legs behave like identical PP plates. As for the 1/8, 1/4 and 3/4-span stress distributions, also identical in the PP plates and PR columns, they are still highly non-linear (like in the P columns). Moreover, they are practically coincident at 1/8 and 1/4-span and slightly more “flat” at 3/8-span – this “flattening” rapidly increase as the mid-span cross-section is approached.
- (iv) The significant difference between the PR and P column post-buckling behaviours is due to the bending (predominantly minor axis) effects occurring in the latter. Although most of these bending effects probably stem from an “effective centroid shift” (*e.g.*, [23]), its value should be determined on the basis of the P column stresses (see fig. 5(a)), and not on the PP plate ones.

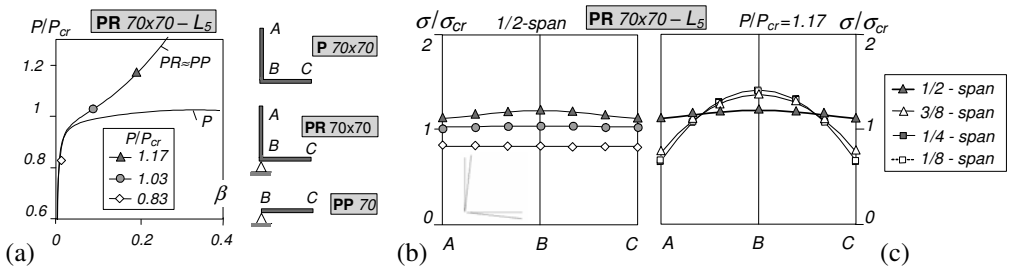


Figure 8: L_5 : (a) PP plate, and PR and P column P/P_{cr} vs. β equilibrium paths, and PP plate and PR column normal stress (b) evolution at mid-span and (c) variation between the 1/8 and mid-span cross-sections ($P/P_{cr}=1.17$).

Next, one investigates how fixing the end sections (warping and flexural rotations prevented) affects the post-buckling behaviour of angle column (F 70×70) with short-to-intermediate lengths (L_3 to L_{11}). Figures 9(a)-(b) show the upper parts of the column post-buckling equilibrium paths P/P_{cr} vs. β and P/P_{cr} vs. d/t , while figure 9(c) displays the L_3 and L_{10} column deformed configuration at two β values. Besides two equilibrium paths also included in figure 9(a), figure 10 presents the L_3 and L_{10} mid and 1/8-span cross-section deformed configurations. Figures 11 and 12 provide the mid-span evolution and longitudinal variation of the L_3 and L_{10} column normal stress distribution (the stresses plotted correspond to the equilibrium states indicated). Finally, figure 13 compares the post-buckling behaviours of the L_{10} F column and those of the corresponding (i) restrained column (FR) and (ii) fixed plate (FP – fixed transverse edges, one longitudinal free edge and the other pinned) – qualitatively similar results were obtained for other column lengths. The observation of all these post-buckling results prompts the following comments:

- (i) As in the pinned-ended columns, there are two types fixed-ended column equilibrium paths, each corresponding to different post-buckling behaviours: (i₁) the L_3 - L_8 columns are clearly stable (fairly high post-critical strength) and exhibit minute mid-span cross-section shear centre displacements, and (i₂) the L_9 - L_{11} columns are barely

- stable, exhibit abrupt limit points (occurring for decreasing rotations and, in columns L_{10} and L_{11} , associated with well-defined “snap-back” phenomena) and involve significant mid-span shear centre displacements.
- (ii) In the longer L_9 - L_{11} columns (like in the pinned-ended L_5 - L_8 columns), the flexural-torsional deformed configuration “switches” abruptly at the peak load: in this case, from two to four half-waves (see fig. 9(c₂)). The peak load and “deformed configuration switch” occur for gradually smaller β values as the column length increases ($L_9 \rightarrow L_{11}$), while the amplitude of the “snap-back” phenomenon drops (it does not even occur for the L_{11} column) – note that the “snap-back” phenomenon causes a “kink” limit point in the P/P_{cr} vs. d/t path. The L_{11} column, corresponding to the transition between (major axis) flexural-torsional and (minor axis) flexural buckling, has “smooth” P/P_{cr} vs. β and P/P_{cr} vs. d/t equilibrium paths – the former exhibits a rather premature well defined limit point and the latter is “almost horizontal”.
 - (iii) All the (shorter) L_3 - L_8 columns, which buckle in pure torsional modes, exhibit a fairly high post-critical strength that decreases with the length ($L_3 \rightarrow L_8$). This fact confirms Rasmussen’s assertion that these columns buckle locally (*i.e.*, to view mode 4 as “local”). Recall that L_4 was the only pinned-ended column buckling in a pure torsional mode and that it exhibited a quite moderate post-critical strength, no limit point and considerable shear centre (flexural) displacements. This seems to indicate that fixing the column end sections significantly (iii₁) increases the susceptibility to pure torsional buckling and (iii₂) restrains the development of flexural displacements, thus contributing decisively to reduce the corresponding destabilising effect.
 - (iv) The GBT modal features provide again an explanation for the differences between the shorter and longer column post-critical strength. The modal participation diagram of figure 1(b₂) shows that the two types of post-buckling behaviour are linked with the absence (L_3 - L_8 columns) or presence (L_9 - L_{11} columns) of deformation mode 2 (major axis flexure) in the column buckling mode. As in the pinned-ended columns, the participation of this mode has a destabilising effect on the post-buckling behaviour of the longer (intermediate) columns.
 - (v) The mid-span normal stresses distribution evolution for $P/P_{cr} > 0.8$ is quite different in the pinned and fixed columns: the latter (v₁) are practically linear in both legs and (v₂) “shift” from the leg edges towards the corner – a behaviour more akin to that usually attributed to angle columns (*e.g.*, [10]).
 - (vi) Restraining the column corner displacements has again a strong impact on the longer column post-buckling behaviour. Indeed, the FR and PR column behaviours are practically identical – and the same happens with the FP and PP plates. The comparison between figures 8 and 13 shows that they only differ in the amount of post-critical strength, which is due to the length difference: 700cm (L_{10} FR column) against 133cm (L_5 PR column).

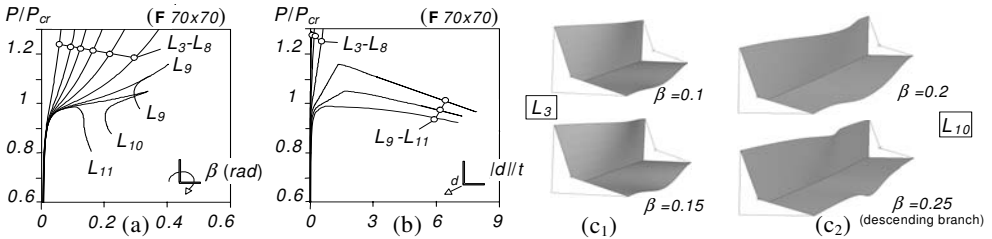


Figure 9: Fixed-ended columns: (a) P/P_{cr} vs. β and (b) P/P_{cr} vs. d/t equilibrium paths, and (c) column deformed configurations of the (c₁) L_3 and (c₂) L_{10} columns at two equilibrium states.

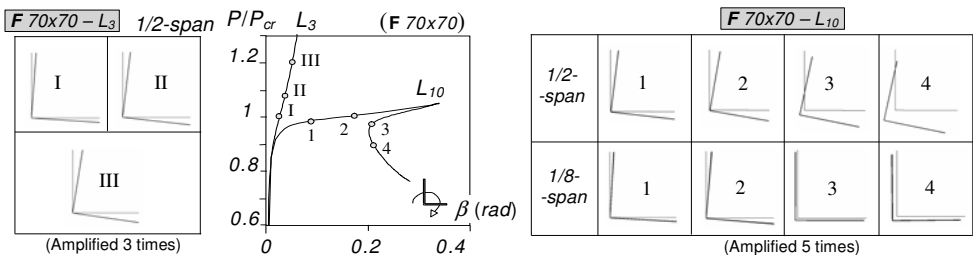


Figure 10: L_3 and L_{10} column: P/P_{cr} vs. β paths and cross-section deformed configuration evolution.

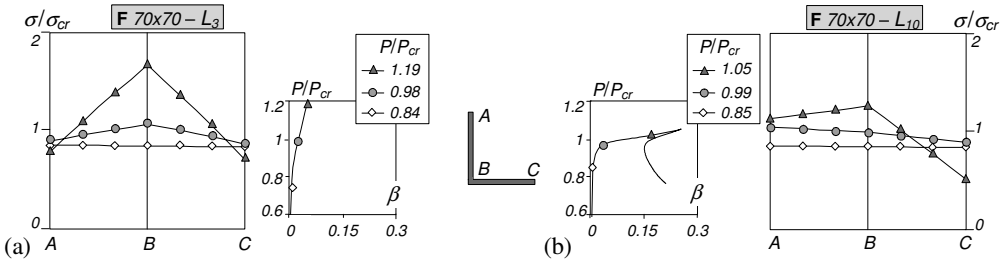


Figure 11: Evolution of the mid-span normal stresses at the of the fixed-ended (a) L_3 and (b) L_{10} columns.

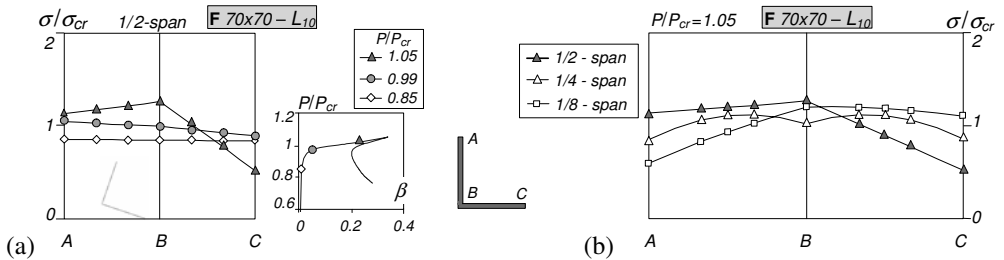


Figure 12: L_{10} column normal stress distribution (a) mid-span normal evolution and (b) longitudinal variation between the 1/8 and mid-span cross-sections ($P/P_{cr}=1.05$).

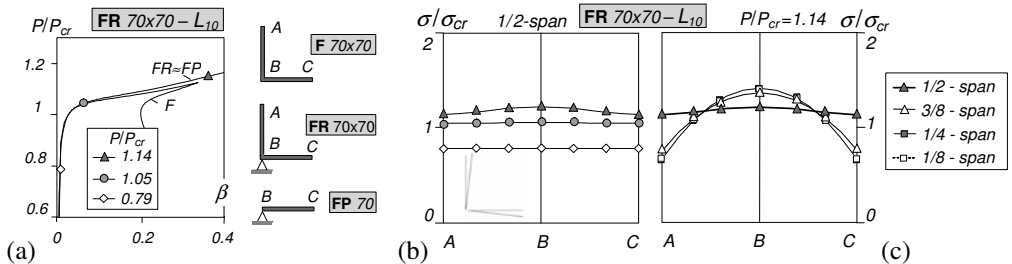


Figure 13: L_5 : (a) PP plate, and PR and P column P/P_{cr} vs. β equilibrium paths, and FP plate and FR column normal stress (b) evolution at mid-span and (c) variation between the 1/8 and mid-span cross-sections ($P/P_{cr}=1.14$).

3.2 Elastic-plastic strength

This section briefly addresses the elastic-plastic strength of pinned and fixed-ended short-to-intermediate angle columns. The results presented concern columns with (i) critical-mode imperfection and $0,1t$ amplitudes, and (ii) four yield-to-critical stress ratios ($f_y/\sigma_{cr} \approx 1.3, 2.5, 5.0, 9.8$, corresponding to $f_y = 30, 60, 120, 235 \text{ MPa}$ and “average” $\sigma_{cr} = 24 \text{ MPa}$) – note that, in order to cover a wide slenderness $\bar{\lambda} = (f_y/\sigma_{cr})^{0.5}$ range, some unrealistically small yield stresses were considered. Figures 14(a)-(b) show the variation of the ultimate load ratio P_u/P_y with the slenderness for the P (L_1-L_8) and F (L_3-L_{11}) columns – it is possible to draw the following conclusions:

- (i) Due to the quite small variation (drop) of σ_{cr} with L within each column set (see fig. 1(a)), the values concerning the columns exhibiting the same yield stress are clearly “grouped together”. As f_y increases, the corresponding group is associated with a higher slenderness and lower strength (*i.e.*, moves to the right and down) – within each group, slenderness increases with the length.
- (ii) The variation of P_u/P_y with $\bar{\lambda}$ within each column group is markedly different for the P and F columns. While the P column values are rather “packed together”, those concerning the F columns exhibit a high “vertical dispersion”, thus implying a very significant variation of P_u/P_y with L (even if σ_{cr} remains practically unaltered). This behavioural difference should be reflected in an efficient design procedure for equal-leg angle columns.

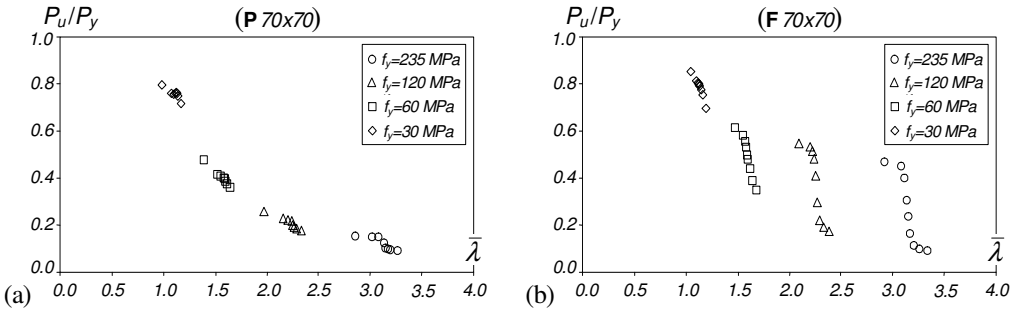


Figure 14: Variation of P_u/P_y with $\bar{\lambda}$ for: (a) pinned-ended and (b) fixed-ended columns angles

- (iii) In spite of the quite pronounced qualitative and quantitative differences detected in the elastic post-buckling behaviours of the L_I - L_8 P columns, the differences between their ultimate strengths are only moderate – note that only the values corresponding to the (very short) L_I columns are outside of the various “packs”.
- (iv) Conversely, the differences between the ultimate strengths of the L_3 - L_{11} F columns are rather sharp – indeed, most of them are located in “almost vertical line segments”, thus meaning that columns sharing the same yield and critical stresses (but having different lengths) exhibit quite distinct P_u/P_y values (e.g., for $f_y=235$ MPa the relation between the higher and lower values exceeds 5.25). This somewhat “paradoxical” behaviour appears to indicate that the slenderness value does not “measure” adequately the column ultimate strength. Recalling that most of these columns buckle in a pure torsional mode akin to a local mode (see fig. 1(b₂)), it seems fair to say that, within this length range, the column ultimate strength nature “travels” from “local” to “global” as the length increases – an efficient design procedure for these columns must take this fact into account.

4 CONCLUSION

This paper reported the results of an ongoing numerical investigation on the (i) elastic buckling and (mostly) post-buckling behaviour and (ii) elastic-plastic strength of short-to-intermediate pinned and fixed-ended equal-leg angle steel columns. The post-buckling and ultimate strength results presented were obtained through ABAQUS shell finite element analyses. Moreover, in order to clarify the distinction between local and global buckling, some GBT-based critical stresses and buckling mode shapes were also displayed and interpreted. Among the various conclusions drawn from this study, the following ones deserve to be specially retained:

- (i) Both the P and F columns exhibit well defined critical stress “plateaus” that correspond to either (i₁) local-torsional, (i₂) torsional or (i₃) flexural-torsional buckling – torsional modes occur mostly in F columns.
- (ii) Within the above “plateaus”, both the P and F pinned columns exhibit quite different elastic post-buckling behaviours, ranging from “local” to “global” (high and low post-critical strength). The amount of corner (shear centre) flexural displacements occurring in the column plays a key role in separating the various behaviours.
- (iii) Within the length range under consideration, the few results obtained appear to indicate that the slenderness value is not adequate to “measure” the column ultimate strength. Further studies are required to confirm this finding, which is bound to have far-reaching implications in the design of equal-leg angle columns.

REFERENCES

- [1] Kitipornchai S. and Chan S.L., “Nonlinear finite-element analysis of angle and tee beam-columns”, *Journal of Structural Engineering* (ASCE), **113**(4), 721-739, 1987.
- [2] Kitipornchai S., Albermani F.G.A. and Chan S.L., “Elastoplastic finite-element models for angle steel frames”, *Journal of Structural Engineering* (ASCE), **116**(10), 2567-2581, 1990.
- [3] Popovic D., Hancock G.J. and Rasmussen K.J.R., “Axial compression tests of cold-formed angles”, *Journal of Structural Engineering* (ASCE), **125**(5), 515-523, 1999.

- [4] Popovic D., Hancock G.J. and Rasmussen K.J.R., “Compression tests on cold-formed angles loaded parallel with a leg”, *Journal of Structural Engineering* (ASCE), **127**(6), 600-607, 2001.
- [5] Trahair N.S., “Lateral buckling strengths of steel angle section beams”, *Journal of Structural Engineering* (ASCE), **129**(6), 784-791, 2003.
- [6] Trahair N.S., “Buckling and torsion of steel unequal angle beams”, *Journal of Structural Engineering* (ASCE), **131**(3), 474-480, 2005.
- [7] Mohan S.J., Rao N.P. and Lakshmanan N., “Flexural and local buckling interaction of steel angles”, *International Journal of Structural Stability and Dynamics*, **5**(2), 143-162, 2005.
- [8] Young B., “Tests and design of fixed-ended cold-formed steel plain angle columns”, *Journal of Structural Engineering* (ASCE), **130**(12), 1931-1940, 2004.
- [9] Ellobody E. and Young B., “Behavior of cold-formed steel plain angle columns”, *Journal of Structural Engineering* (ASCE), **131**(3), 457-466, 2005.
- [10] Rasmussen K.J.R., “Design of angle columns with locally unstable legs”, *Journal of Structural Engineering* (ASCE), **131**(10), 1553-1560, 2005.
- [11] Rasmussen K.J.R., “Design of slender angle section beam-columns by the direct strength method”, *Journal of Structural Engineering* (ASCE), **132**(2), 204-211, 2006.
- [12] Schafer B.W., “Review: the direct strength method of cold-formed steel member design”, *Journal of Constructional Steel Research*, **64**(7-8), 766-778, 2008.
- [13] Chodraui G.M.B., Shifferaw Y., Malite M. and Schafer B.W., “Cold-formed steel angles under axial compression”, *Proceedings of 18th International Specialty Conference on Cold-Formed Steel Structures* (Orlando, 26-27/10), R. LaBoube, W.W. Yu (eds.), 285-300, 2006.
- [14] Chodraui G.M.B., Shifferaw Y., Malite M. and Schafer B.W., “On the stability of cold-formed steel angles under compression”, *REM – Revista Escola de Minas* (Brazil), **60**(2), 355-363, 2007. (Portuguese)
- [15] Dinis P.B., Camotim D. and Silvestre N., “On the local and global buckling behaviour of angle, T-section and cruciform thin-walled columns and beams”, *Thin-Walled Structures*, accepted for publication, 2010.
- [16] Dinis, P.B., Silvestre, N. and Camotim D., “On the local and global post-buckling behaviour and strength of thin-walled angle columns and beams”, *Book of Abstracts of 7th European Solid Mechanics Conference* (ESMC 2009 – Lisboa, 7-11/9), J. Ambrósio, M. Silva (eds.), 649-650, 2009.
- [17] Dinis P.B., Silvestre N. and Camotim D., “Buckling and post-buckling behaviour of angles”, *Proceedings of VII National Congress on Steel and Composite Structures* (Lisboa, 18-19/11), L.S. Silva *et al.* (eds.), II-269-278, 2009. (Portuguese)
- [18] Simulia Inc., *ABAQUS Standard* (vrs. 6.7-5), 2008.
- [19] Dinis P.B., Camotim D. and Silvestre N., “FEM-based analysis of the local-plate/distortional mode interaction in cold-formed steel lipped channel columns”, *Computers & Structures*, **85**(19-20), 1461-1474, 2007.
- [20] Dinis P.B. and Camotim D., “On the use of shell finite element analysis to assess the local buckling and post-buckling behaviour of cold-formed steel thin-walled members”, *Book of Abstracts of III European Conference on Computational Mechanics: Solids, Structures and Coupled Problems in Engineering* (III ECCM – Lisboa, 5-9/6), C.A.M. Soares *et al.* (eds.), Springer, 689, 2006. (full paper in CD-ROM Proceedings)
- [21] Bebiano R., Silvestre N. and Camotim D., *GBTUL 1.0 β - Code for Buckling and Vibration Analysis of Thin-Walled Members*, freely available at <http://www.civil.ist.utl.pt/gbt>, 2008.
- [22] Bebiano R., Silvestre N. and Camotim D., “GBTUL – a code for the buckling analysis of cold-formed steel members”, *Proceedings of 19th International Specialty Conference on Recent Research and Developments in Cold-Formed Steel Design and Construction* (St. Louis, 14-15/10), R. LaBoube, W.W. Yu (eds.), 61-79, 2008.
- [23] Young B. and Rasmussen K.J., “Shift of effective centroid in channel columns”, *Journal of Structural Engineering* (ASCE), **125**(5), 524-531, 1999.